

Synthesis and Optical Properties of Bismuth-based Perovskite Materials

Yunhe Li

School of Chemistry and Chemical Engineering, Qufu Normal University, Jining, 273100, China
liyunhe102826@outlook.com

ABSTRACT

Bismuth-based perovskite has become the best candidate material for non-lead perovskite because of its low toxicity and good moisture stability. The structural diversity of bismuth halide perovskites gives them many photoelectric properties, such as nonlinear optical properties, photochromic effects and photoelectric effects. However, bismuth halide perovskite materials with different stoichiometric ratios have different light absorption properties and carrier transport processes. In order to search for high stability and excellent optical properties of bismuth halide perovskite materials, this paper synthesized Rb₃BiBr₆ materials by using rubidium bromide and bismuth bromide as precursors, and further studied the morphology and optical properties of the materials by scanning electron microscopy, UV-VIS absorption spectroscopy, ultraviolet photoelectron spectroscopy and nanosecond transient absorption spectroscopy. The results show that the material has a wide light absorption range and a long carrier transfer process, indicating that the bismuth-based perovskite material has great application value in the field of photocatalysis and photodetector.

KEYWORDS

Bismuth-based perovskite material; Optical properties; Carrier; Photocatalysis

1. INTRODUCTION

Recently, bismuth-based perovskite materials have been favored by researchers owing to their excellent environmental stability, low toxicity and good humidity stability, large absorption coefficient ($\sim 10^5 \text{ cm}^{-1}$), and have become the best candidate materials for toxic lead-based perovskite [1]. Bismuth halide perovskite is an environmentally sustainable semiconductor with outstanding stability under atmospheric pressure and wet conditions compared to Sn or Ge based perovskite. CsBi₃I₁₀ has been studied for its excellent performance in stability and electronic properties, and is expected to become a bismuth-based perovskite material for photoelectrical applications [2]. The trivalent bion electron configuration of bismuth is equal to that of lead ion (6s6p), which can be made up for the intrinsic defect state of lead and enable bismuth-based perovskite materials to have a long carrier lifetime [3]. In addition, the structural diversity of bismuth halide perovskites also gives them outstanding photoelectric properties, such as nonlinear optical properties, thermal, photochromic and photoelectric effects [4]. Among them, bismuth-based zero-dimensional perovskites show great application prospects in photovoltaic field due to the influence of intrinsic quantum and dielectric limiting effects. At present, studies mainly focus on the preparation of zero-dimensional bismuth halide perovskites by cation regulation of highly toxic organic amines or heterocyclic organic amines, while few studies have been conducted on the solid-state light emission properties of bismuth halide perovskites. Moreover, the photoluminescence properties of perovskites largely depend on bismuth halide cluster units. Therefore, new environmentally friendly cations are used to regulate the luminous

properties of zero-dimensional bismuth halide clusters and that is of great significance for the application and development of non-lead perovskite materials [5].

Bismuth-based perovskites exhibit different photoelectric properties due to the diversity of their structures. Cs^+ , Bi^{3+} and Br^- can form a number of compounds with different stoichiometric and crystal structures, such as CsBiBr_4 , CsBi_2Br_7 , $\text{Cs}_3\text{Bi}_2\text{Br}_9$ and Cs_3BiBr_6 , among which $\text{Cs}_3\text{Bi}_2\text{Br}_9$ and Cs_3BiBr_6 exist stably in air [6]. With the in-depth study of bismuth-based perovskite materials, Tang Jiang et al. synthesized $\text{Cs}_3\text{Bi}_2\text{Br}_9$ quantum dots with bright blue emission and good stability by studying the crystallization mechanism of $\text{Cs}_3\text{Bi}_2\text{Br}_9$ single crystal, and its photoluminescence quantum efficiency was as high as 26.4% [7]. The photoluminescent quantum yield of $\text{Cs}_3\text{Bi}_2\text{Br}_9$ at 410nm is 46%, which is better than other reported halide perovskites. Ou Chen et al. reported a new non-lead zero-dimensional Cs_3BiX_6 perovskite nanocrystal, and demonstrated that Cs_3BiX_6 nanocrystals can be transformed into other bismuth-based perovskite materials through simple anion exchange or metal ion insertions, providing guidance for further understanding of the relationship between the structure and properties of bismuth-based perovskite materials [8]. Han Xiaodong et al. synthesized and controlled the morphology of bismuth-based perovskite nanocrystals by changing the proportion of the precursor and the reaction temperature [9]. Zero-dimensional Cs_3BiCl_6 was used as a template molecule and converted into $\text{Cs}_3\text{Bi}_2\text{Cl}_9$ nanoplates or $\text{Cs}_4\text{MnBi}_2\text{Cl}_{12}$ nanoplates by Cl induced metal ion insertion. This growth mechanism is also applicable to the synthesis of $\text{Cs}_4\text{CdBi}_2\text{Cl}_{12}$ nanosheets. In addition, the alloying of Cd^{2+} in $\text{Cs}_4\text{MnBi}_2\text{Cl}_{12}$ lattice can weaken the strong coupling effect between Mn and Mn, thus extending the photoluminescence lifetime and increasing the photoluminescence quantum yield. These results provide new research ideas for the synthesis of bismuth-based perovskite nanocrystals and their applications in photodetectors and radiation detectors.

As mentioned above, this paper, based on the synthesis of Rb_3BiBr_6 materials, various optical properties of bismuth-based perovskite materials were analyzed. The optical properties of the materials were studied by powder X-ray diffraction, scanning electron microscope, thermogravimetric analyzer, ultraviolet photoelectron spectroscopy, UV-VIS diffuse reflection spectrometer and nanosecond transient absorption spectra. The results show that the material has a high visible light absorption range, indicating that it has potential application value in the field of photocatalysis and photodetectors.

2. METHODOLOGY

2.1. Material Preparation

Rb_3BiBr_6 was synthesized in an autoclave using 3 mmol of RbBr (99.8%) and 1 mmol of BiBr_3 (98%) as precursors. After cooling, remove the test tube, extract the upper liquid with an eyedropper, place the crystal in the oven for drying, and then grind it with a mortar to obtain Rb_3BiBr_6 powder.

2.2. Optical Test

The morphology, structure, and optical properties of Rb_3BiBr_6 were characterized via powder X-ray diffraction (XRD), scanning electron microscope (SEM), thermogravimetric analyzer (TG), ultraviolet photoelectron spectroscopy (UPS), and UV-VIS-DRS. The morphology and structure of the materials were controlled by regulating the process parameters of the synthesis method.

3. RESULTS AND DISCUSSION

3.1. XRD Characterization

Single crystal X-ray diffraction was employed to examine the fabricated Rb_3BiBr_6 perovskite material. The outcomes (Fig. 1a, 1b, 1c) indicate that the Rb_3BiBr_6 material possesses an octahedral configuration with Bi as the central atom and Br as the ligand, while Rb atoms are distributed in the horizontal direction of the octahedron, constituting a zero-dimensional structure. The cell parameters are $a=13.1882 \text{ \AA}$, $b=26.4383 \text{ \AA}$, $c=8.5807 \text{ \AA}$ and $\alpha = \beta = \gamma = 90^\circ$. The powder XRD pattern (Fig.1d) reveals that the prepared sample aligns with the simulated XRD diffraction peaks. The aforementioned results verify that the Rb_3BiBr_6 perovskite material has been successfully synthesized.

Table 1. Structural parameters of Rb_3BiBr_6 nanocrystals

| | |
|--------------------|----------------------------|
| Compound | Rb_3BiBr_6 |
| Formula weight | 944.85 |
| Temperature/K | 150 |
| Hall group | -P 2ac 2n |
| Space group | Pn ma |
| a | 13.1882 \AA |
| b | 26.4383 \AA |
| c | 8.5807 \AA |
| α | 90o |
| β | 90o |
| γ | 90o |
| $V= \text{ \AA}^3$ | 2991.86 (7) |
| Z | 8 |
| F (000) | 3232.0 |
| hmax | 15 |
| kmax | 32 |
| lmax | 10 |

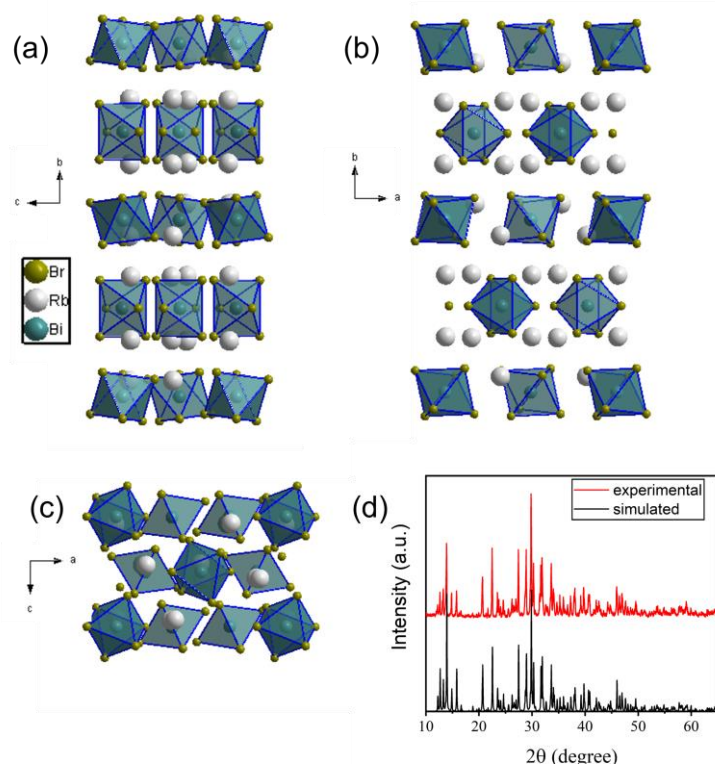


Figure 1. (a, b, c) Structure diagram of Rb_3BiBr_6 nanocrystals; (d) XRD pattern of Rb_3BiBr_6

3.2. SEM Characterization

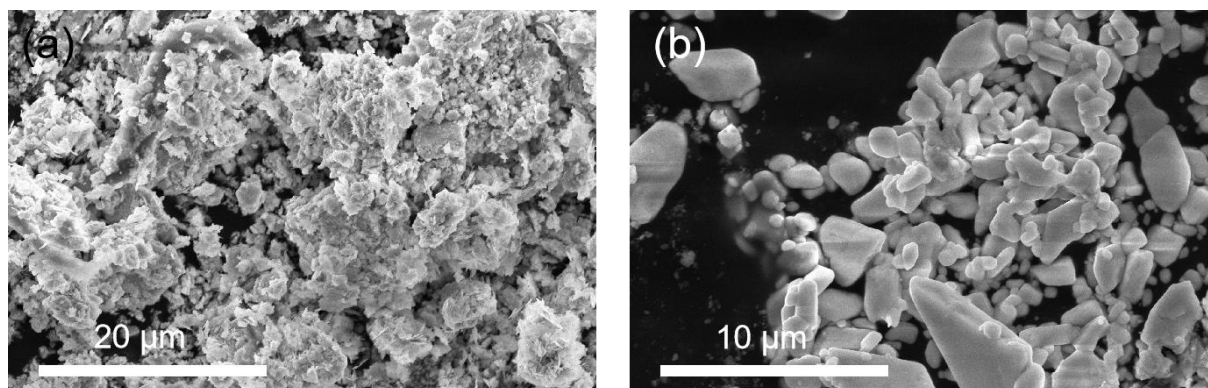


Figure 2. (a, b) Scanning electron microscopy of Rb_3BiBr_6

The morphology of Rb_3BiBr_6 materials can be observed by scanning electron microscopy. Fig.2a shows that the material morphology is irregular blocky and tightly arranged, and the surface is covered with densely packed particles of different sizes and shapes. A bright smooth boundary with a clear structure and a particle size of about 5 microns can be observed in the SEM image with high magnification (Fig. 2b). The results show that Rb_3BiBr_6 has good crystallinity.

3.3. Thermogravimetric Analysis Characterization

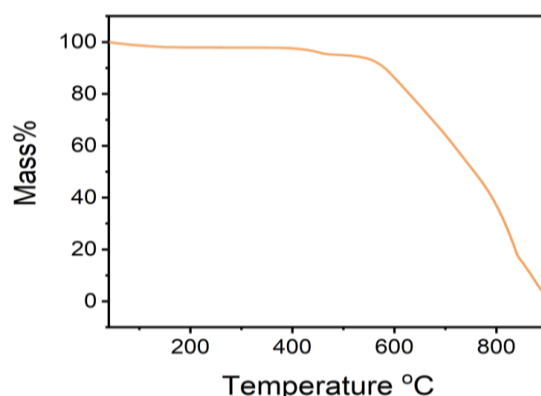


Figure 3. Thermogravimetric analysis diagram of Rb_3BiBr_6

Thermal stability is an important parameter to evaluate the properties of materials. The higher the thermal stability of materials, the better the application of materials in thermal catalysis and photocatalysis. The stability of Rb_3BiBr_6 perovskite was studied by thermogravimetric analysis. As shown in Fig.3, the results show that the first mass loss (2.9%) occurs at 500°C, which is attributed to the volatilization of a small amount of bromine element. When the temperature rises to 580°C, the mass fraction drops sharply, indicating that the Rb_3BiBr_6 material begins to decompose. The above results show that Rb_3BiBr_6 perovskite material has excellent thermal stability.

3.4. Uv Photoelectron Spectroscopy and Diffuse Reflection Characterization

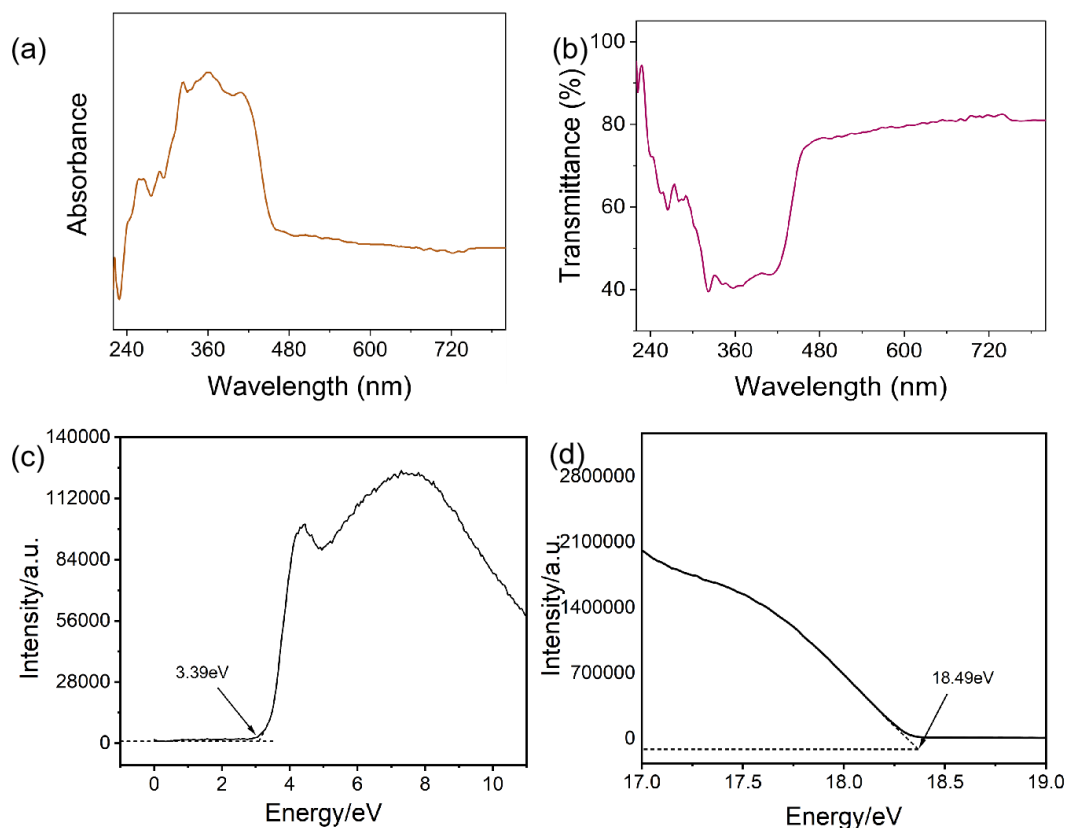


Figure 4. (a) UV-VIS absorption spectrum of Rb_3BiBr_6 ; (b) diffuse reflection spectrum of Rb_3BiBr_6 ; Ultraviolet photoelectron spectra of (c, d) Rb_3BiBr_6

In order to study the valence band and conduction band position of the material and realize the application of the material in the field of photocatalysis, the UV-VIS absorption spectrum and

ultraviolet photoelectron spectrum of the material were measured. As shown in Fig.4a, Rb_3BiBr_6 material exhibits a strong absorption peak in the range of 260~720 nm, indicating that the material can make full use of visible light. In addition, Rb_3BiBr_6 has a strong reflectivity in the ultraviolet region (Fig.4b), suggesting potential applications for the preparation of sunscreens. According to the Kubelka-Munk formula, the band gap size of Rb_3BiBr_6 material is 2.75 eV. Uv photoelectron spectroscopy shows that the difference between the valence band position (E_{vb}) of Rb_3BiBr_6 and the Fermi level (E_{F}) ($E_{\text{VB}}-E_{\text{F}}$) is 3.39 eV (Fig.4c), and the difference between the Fermi level and the vacuum level of Rb_3BiBr_6 is 18.49 eV (Fig.4d). From this, the difference between the Fermi level and the vacuum level value can be calculated as 2.71 eV. According to the above analysis results, it is further obtained that the conduction band position is 2.75 eV. The valence band position relative to the vacuum level is 6.1 eV, and the conduction band position is 3.35 eV (Fig.5). The conduction band position is higher than the hydrogen electrode point position, indicating that the material has potential application value in the field of photocatalytic water decomposition.

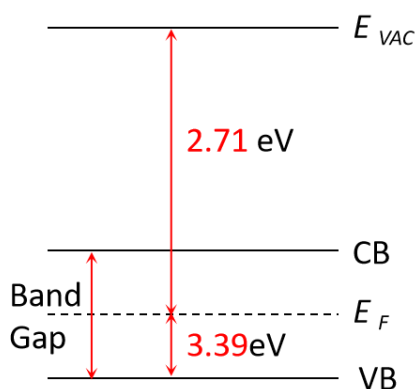


Figure 5. Schematic diagram of valence band and conduction band levels of Rb_3BiBr_6

3.5. Characterization of Nanosecond Transient Dynamics

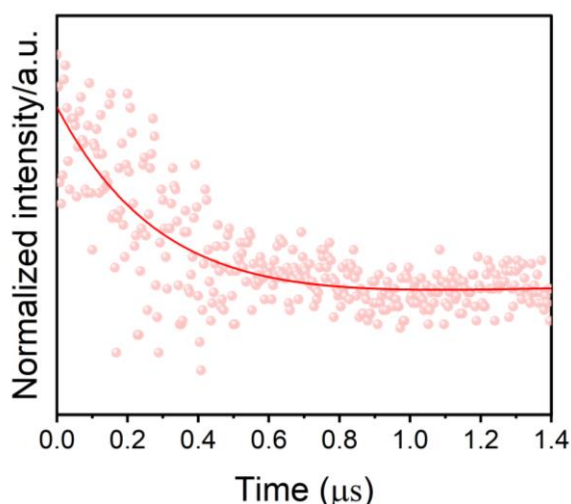


Figure 6. Nanotransient absorption spectra of Rb_3BiBr_6

Nano-transient absorption spectroscopy is an effective tool to analyze the carrier transport process of materials. As shown in Fig.6, we observed the excited state-induced absorption signal during the test and fitted it with a single exponential, which showed a material lifetime of 242 ns. No photoluminescence of the material was observed during the experiment, so this lifetime is attributed to the emission of Rb_3BiBr_6 's secretly trapped excitons [10]. This study further revealed that the material has a long carrier lifetime, which is helpful to realize the application of bismuth-based perovskite materials in the field of photocatalysis.

4. CONCLUSION

In this paper, RbBr and BiBr₃ are used as precursors to synthesize bismuth-based perovskite materials. The crystal structure of the materials is regulated by adjusting the process parameters of the synthesis method, and the crystal quality of the materials is optimized. The morphology, structure and optical properties of the materials were measured by powder X-ray diffraction, scanning electron microscope, thermogravimetric analyzer, ultraviolet photoelectron spectrometer and UV-VIS diffuse reflection spectrometer. The results show that the material has a wide light absorption range, and the conductive band position of the material is suitable for the application of photocatalytic hydrogen evolution. The study process of the carrier dynamics of the material is further analyzed by nanotransient absorption spectroscopy. This study provides a new research idea for the design and application of non-lead perovskite materials.

REFERENCES

- [1] Wang, J., Wang, J., Li, N., et al. (2020). Direct Z-scheme 0D/2D heterojunction of CsPbBr₃ quantum dots/Bi₂WO₆ nanosheets for efficient photocatalytic CO₂ reduction. *ACS Applied Materials & Interfaces*, 12(28), 31477-31485.
- [2] Bi, W., Leblanc, N., Mercier, N., et al. (2009). Thermally induced Bi (III) lone pair stereoactivity: ferroelectric phase transition and semiconducting properties of (MV) BiBr₅ (MV= methylviologen). *Chemistry of materials*, 21(18), 4099-4101.
- [3] Park, B. W., Philippe, B., Zhang, X., et al. (2015). Bismuth Based Hybrid Perovskites A₃Bi₂I₉ (A: Methylammonium or Cesium) for Solar Cell Application. *Advanced Materials (Deerfield Beach, Fla.)*, 27(43), 6806-6813.
- [4] Shi, M., Li, G., Tian, W., et al. (2020). Understanding the effect of crystalline structural transformation for lead-free inorganic halide perovskites. *Advanced Materials*, 32(31), 2002137.
- [5] Lehner, A. J., Fabini, D. H., Evans, H. A., et al. (2015). Crystal and electronic structures of complex bismuth iodides A₃Bi₂I₉ (A=K, Rb, Cs) related to perovskite: aiding the rational design of photovoltaics. *Chemistry of materials*, 27(20), 7137-7148.
- [6] Tran, M. N., Cleveland, I. J., & Aydil, E. S. (2020). Resolving the discrepancies in the reported optical absorption of low-dimensional non-toxic perovskites, Cs₃Bi₂Br₉ and Cs₃BiBr₆. *Journal of Materials Chemistry C*, 8(30), 10456-10463.
- [7] Zhang, J., Yang, Y., Deng, H., et al. (2017). High quantum yield blue emission from lead-free inorganic antimony halide perovskite colloidal quantum dots. *ACS nano*, 11(9), 9294-9302.
- [8] Yang, H., Cai, T., Liu, E., et al. (2020). Synthesis and transformation of zero-dimensional Cs₃BiX₆ (X= Cl, Br) perovskite-analogue nanocrystals. *Nano Research*, 13, 282-291.
- [9] Wang, C., Xiao, J. W., Yan, Z. G., et al. (2023). Colloidal synthesis and phase transformation of all-inorganic bismuth halide perovskite nanoplates. *Nano Research*, 16(1), 1703-1711.
- [10] Zhou, W., Han, P., Zhang, X., et al. (2020). Lead-free small-bandgap Cs₂CuSbCl₆ double perovskite nanocrystals. *The Journal of Physical Chemistry Letters*, 11(15), 6463-6467.